JGV Papers in Press. Published December 9, 2013 as doi:10.1099/vir.0.061986-0

Neutrophils Are Needed for an Effective Immune Response Against Pulmonary Rat Coronavirus Infection, but also Contribute to Pathology

Running Title: Neutrophils in rat coronavirus infection

Contents Category: Animal Viruses- Positive-Strand RNA

Anoria K. Haick[1,2], Joanna P. Rzepka[1,3], Elizabeth Brandon[1], Onesmo B. Balemba[1], and Tanya A. Miura[1*]

[1]Department of Biological Sciences, University of Idaho, 875 Perimeter Dr., MS 3051, Moscow, ID 83844-3051, USA

[2]Current Address: Department of Obstetrics and Gynecology, University of Washington School of Medicine, 1959 Northeast Pacific Street, Seattle, WA 98195, USA

[3]Current Address: Veterinary Medical Research and Development Incorporated, 425 Northwest Albion Drive, Pullman, WA 99163, USA

[*]Corresponding Author. Email: tmiura@uidaho.edu. Telephone: (208)885-4940. Fax: (208)885-7905

Word Count Summary: 234

Word Count Text: 5499

Tables: 2

Figures: 6

Summary

Polymorphonuclear neutrophils (PMN) infiltrate the respiratory tract early after viral infection and can contribute to both host defense and pathology. Coronaviruses are important causes of respiratory tract infections, ranging from mild to severe depending on the viral strain. This study evaluated the role of PMN during a non-fatal pulmonary coronavirus infection in the natural host. Rat coronavirus (RCoV) causes respiratory disease in adult rats, characterized by an early PMN response, viral replication and inflammatory lesions in the lungs, mild weight loss, and effective resolution of infection. To determine their role during RCoV infection, PMN were depleted and the effects on disease progression, viral replication, inflammatory response, and lung pathology were analyzed. Compared to RCoV infection in control animals, PMN-depleted rats had worsened disease with weight loss, clinical signs, mortality, and prolonged pulmonary viral replication. PMN-depleted animals had fewer macrophages and lymphocytes in the respiratory tract, corresponding with lower chemokine levels. Combined with *in vitro* experiments showing that PMN express cytokines and chemokines in response to RCoV-infected alveolar epithelial cells, these findings support a role for PMN in eliciting an inflammatory response to RCoV infection. Despite their critical role in the protection from severe disease, the presence of PMN was correlated with hemorrhagic lesions, epithelial barrier permeability, and cellular inflammation in the lungs. This study demonstrated that while PMN are required for an effective antiviral response, they also contribute to lung pathology during RCoV infection.

Introduction

Inflammatory responses triggered by respiratory viruses are necessary for the initiation of effective antiviral immunity, but can also become dysregulated and result in acute lung injury and respiratory distress syndrome. Polymorphonuclear neutrophils (PMN) infiltrate the airways early after infection by respiratory viral pathogens including rhinoviruses, influenza viruses, respiratory syncytial virus, and coronaviruses. The presence of PMN in the respiratory tract during viral infection is frequently correlated with clinical symptoms or severe disease pathology (Bradley *et al.*, 2012; Denlinger *et al.*, 2011; Khanolkar *et al.*, 2009; McKean *et al.*, 2003; Nagata *et al.*, 2008; Tumpey *et al.*, 2005). In contrast, PMN have direct antiviral activities and also function in the activation of innate and adaptive immune responses, and thus can contribute to effective antiviral responses (Mantovani *et al.*, 2011; Tate *et al.*, 2012; Tate *et al.*, 2011; Widegren *et al.*, 2011). Because PMN can be involved in both protective and pathologic immune responses, a complete understanding of their functions during viral infection may lead to the design of therapeutic strategies that exploit the beneficial functions of PMN while limiting their damaging effects in the lung.

Coronaviruses (CoV) cause respiratory diseases in humans as well as companion and agricultural animals. Human CoV infections may result in mild common colds, more serious lower respiratory tract diseases, or the highly fatal severe acute respiratory syndrome (SARS) or Middle East Respiratory Syndrome (MERS), depending on the virus strain and the age and immune status of the host (Assiri *et al.*, 2013; Gaunt *et al.*, 2010; Lee *et al.*, 2003). PMN are recruited to CoV-infected tissues, and either contribute to pathology or are necessary for an effective immune response, depending on the specific CoV and disease model. The presence of PMN corresponds to increased disease severity in humans and animals infected with SARS-CoV

or human CoV-229E (Leong *et al.*, 2006; McKean *et al.*, 2003; Nagata *et al.*, 2008; Tsui *et al.*, 2003). During neurotropic murine coronavirus infection, PMN contribute to brain pathology (Iacono *et al.*, 2006), but are also critical for the effective resolution of infection by promoting blood-brain barrier permeability, which is needed for effective T cell recruitment to the brain (Hosking *et al.*, 2009; Zhou *et al.*, 2003). Despite these findings and the fact that CoVs commonly infect the respiratory tract, the functions of PMN during respiratory CoV infections are not well understood.

Rodent models of respiratory coronavirus infection are available for SARS-CoV, but not the more common and milder CoV that circulate in human populations worldwide. We have developed a rat coronavirus (RCoV) model to determine the mechanisms that promote effective resolution of a non-fatal coronavirus infection in the lung. RCoV is a natural pathogen of rats that replicates and causes mild disease in the upper and lower respiratory tracts (Funk *et al.*, 2009; Wojcinski & Percy, 1986). Intratracheal inoculation of adult rats with RCoV results in viral replication in the type I alveolar epithelial (AT1) cells in the lung, recruitment of PMN into the respiratory tract, expression of PMN chemotactic chemokines, and transient, focal pneumonitis (Funk *et al.*, 2009). The virus and inflammatory infiltrates within the alveoli are resolved by day 8 after infection, suggesting the rapid development of an effective antiviral response to infection. The role of PMN in this effective response to RCoV infection is not known. In this study, PMN recruitment to the lungs of RCoV-infected rats was inhibited using antibody-mediated depletion to determine the role of PMN in viral clearance, lung pathology, and disease severity.

Results

PMN depletion enhances RCoV-mediated disease.

There is robust recruitment of PMN to the respiratory tract during RCoV infection (Funk *et al.*, 2009). To delineate their role during infection, rats were injected with rabbit anti-rat PMN serum (αPMN) one day prior to intranasal inoculation of virus. Depletion was maintained by t injections of αPMN every 48 h (Fig. 1a). Control rats were injected with normal rabbit serum (NRS) on the same schedule. Several previous studies have used this polyclonal αPMN antibody to effectively deplete circulating PMN in rats without significantly altering other white blood cell populations (Janardhan *et al.*, 2006; Li *et al.*, 2007; Ofulue & Ko, 1999; Sir *et al.*, 2000; Snipes *et al.*, 1995). In agreement with these studies, αPMN effectively and specifically depleted PMN from the blood of rats for at least 4 days, followed by re-population by day 6 post-infection (Fig. 1b). Importantly, αPMN serum did not reduce the numbers of other white blood cell types in RCoV-infected or uninfected animals (Fig. 1b and Supplemental Fig. 1). Thus, αPMN is an effective, specific tool for transient depletion of circulating PMN in rats.

PMN-depleted and NRS-treated animals were inoculated with RCoV and weighed and observed daily for clinical signs and mortality. In agreement with our previous study, RCoV infection of NRS-treated rats did not result in mortality (Funk *et al.*, 2009). In contrast, treatment with αPMN resulted in 28% mortality of RCoV-infected rats by day 6 (Fig. 1c). Of the 18 rats in the αPMN/RCoV group, 1 succumbed to infection on day 2 and 4 others were humanely euthanized due to excessive weight loss and severe disease. None of the mock-infected animals, either with or without αPMN treatment, died or required euthanasia during the course of the experiment. All of the treatment groups exhibited weight loss early in the study and, except for

the αPMN/RCoV group, steadily regained weight beginning on day 3 (Fig. 1d). In contrast, PMN-depleted rats that were infected with RCoV had steady weight loss through day 4, which remained low through day 8 (Fig. 1d). Clinical scores were calculated daily as described in materials and methods (Fig. 1e). NRS-treated rats infected with RCoV showed no or only minor clinical signs during infection. In contrast, RCoV infection of αPMN-treated rats resulted in multiple clinical signs, including hunched posture, ruffled fur, swollen face and neck, bloody eye and nasal discharge, and lethargy. Therefore, these rats had significantly increased mean clinical scores between days 1 and 8 post-infection (Fig. 1e). Surviving animals (72%) had lower clinical scores after day 4, but did not return to complete health by day 8. The increased morbidity and mortality in rats treated with αPMN, which specifically depletes PMN from the bloodstream, suggests that PMN are needed for protection against severe disease during RCoV infection.

αPMN treatment reduces PMN recruitment and prolongs viral replication in the lungs.

To confirm that treatment with αPMN inhibits recruitment of PMN to the respiratory tract, PMN were quantified in bronchoalveolar lavage fluid (BALF) on days 4, 8, and 12 post-infection. As expected from our previous study (Funk *et al.*, 2009), PMN numbers increased in NRS/RCoV-treated rats by day 4, and declined to less than 5% by day 8 (Fig. 2a). In rats treated with αPMN, PMN numbers in the BALF did not increase upon RCoV infection and remained low through day 12, despite their repopulation of the blood by day 6 (Fig. 1b). To determine whether PMN are needed for clearance of RCoV, viral titers from lung homogenates were compared in NRS- and αPMN-treated rats. Both groups had high levels of RCoV on day 4, which remained high in αPMN-treated rats through day 12 (Fig. 2b). In contrast, NRS-treated

rats cleared the virus by day 8 post-infection. Thus, recruitment of PMN to the respiratory tract correlated with effective clearance of RCoV from the lungs.

PMN are needed early during RCoV infection to protect against disease.

PMN are observed in the respiratory tract early after infection with RCoV (Funk *et al.*, 2009), but it is not known if their presence early during infection is important to later disease outcomes. To establish transient depletion of PMN early during RCoV infection, rats were treated with αPMN serum one day before and two days after RCoV inoculation (Fig. 3a). No PMN were detected in the BALF of αPMN-treated rats on day 4 post-infection, followed by recruitment of PMN to the respiratory tract by day 8 (Fig. 3b). Despite the influx of PMN into the airways, viral titers in the lungs remained high on day 8 (Fig. 3c), suggesting that the presence of PMN alone is not sufficient to clear virus late in infection. Transient PMN depletion resulted in 50% mortality by day 8 after RCoV infection and significant weight loss compared to NRS-treated animals (Fig. 3d and e). NRS-RCoV rats initially lost weight, which they re-gained after day 3 (Fig. 3e). Of the 6 animals that died during the study, 1 succumbed to infection on day 3 and 5 were euthanized due to more than 20% weight loss and severe disease. Clinical signs were apparent on days 2-8 post-infection and were identical to those seen in rats given αPMN throughout infection (Data not shown). These findings demonstrate that delayed recruitment of PMN to the lungs cannot compensate for their absence early during RCoV infection.

PMN promote pulmonary cellular infiltration during RCoV infection.

153 The results of transient PMN depletion suggested that PMN are needed early during
154 RCoV infection to limit disease severity, and that later recruitment of PMN does not reduce viral
155 titers. Therefore, we hypothesize that PMN have an indirect role in the effective response against
156 RCoV infection. RCoV infection induces cellular infiltration into the alveolar spaces (Funk *et*
157 *al.*, 2009). To determine whether PMN are required for cellular inflammation, histological
158 analysis of lung tissues was performed on PMN-depleted and NRS-treated rats during RCoV
159 infection. Focal areas of pneumonitis with PMN, macrophages, and lymphocytes were present in
160 the lung sections from NRS-treated, but not αPMN-treated, animals on day 4 post-infection (Fig.
161 4a). Inflammatory lesions in the lungs of NRS-treated animals were mostly localized in areas
162 surrounding the bronchioles (top panels). Quantitative analysis of density indices of PMN,
163 macrophages, and lymphocytes was performed on tissue sections from three animals per group.
164 αPMN treatment significantly reduced the numbers of macrophages and lymphocytes in the
165 lungs of RCoV infected animals (Fig. 4b), corresponding with cell counts in BALF samples (Fig.
166 4c). To determine whether CD4 or CD8 positive lymphocytes were specifically reduced, these
167 cells were quantified in BALF by flow cytometry. This analysis demonstrated a reduction in both
168 CD4 and CD8 positive cells in the airways of αPMN-treated animals, compared to NRS-treated
169 animals, upon RCoV infection (Fig. 4d). These data suggest that PMN are critical for the
170 development of a cellular response to pulmonary RCoV infection.

171

172 **☐PMN-treated rats have reduced chemokine concentrations in the BALF during RCoV**

173 **infection.**

The histology data demonstrated that PMN promote pulmonary cellular infiltration during RCoV infection, and our previous studies showed RCoV-induced chemokine expression (Miura *et al.*, 2007)(Funk *et al.*, 2009). To determine whether PMN contribute to this response, we quantified chemokines in the BALF of αPMN and NRS-treated rats during RCoV infection. Compared to mock-inoculated animals, RCoV infection increased levels of PMN-specific chemokines (CXCL-1 and CXCL-3) in NRS-treated animals by day 4, which returned to mock levels by day 8 (Fig. 5a). In contrast, PMN-depleted rats had significantly reduced levels of CXCL-1 and CXCL-3 in the BALF, which corresponded with the lack of PMN recruitment to the lungs of depleted animals even after PMN had repopulated the blood (Fig. 1b and 2a). Two additional chemokines that are induced by RCoV infection (Funk *et al.*, 2009), interferon-inducible protein 10 (IP-10/CXCL-10) and monocyte chemoattractant protein 1 (MCP-1/CCL-2), were quantified in BALF from αPMN and NRS treated rats on day 4 post-infection (Fig. 5b). Both chemokines were induced by RCoV infection in NRS-treated, but not αPMN-treated rats, suggesting that PMN are needed for chemokine production.

Proinflammatory response of PMN to RCoV-infected alveolar epithelial cells *in vitro*.

Based on the data above, we hypothesize that PMN recruited to the airways of RCoV-infected rats produce cytokines and chemokines, including CXCL-1, CXCL-3, IP-10, and CCL-2. Type I alveolar epithelial (AT1) cells are the primary cell type infected by RCoV within the distal lung (Funk *et al.*, 2009). Furthermore, RCoV-infected AT1-like cells direct PMN functions *in vitro* (Rzepka *et al.*, 2012). To determine whether RCoV-infected AT1 cells direct expression of cytokines and chemokines by PMN, we incubated PMN isolated from rat bone marrow in

196 conditioned medium from RCoV-infected (RCoV-AT1) or mock-infected (mock-AT1) AT1-like
197 cells. The mRNA levels of 84 cytokines and chemokines were measured from PMN using
198 quantitative RT-PCR arrays (Table 1). PMN that were incubated in RCoV-AT1 medium had
199 higher mRNA levels of proinflammatory cytokines (IL-18, IL-1α, IL-1β, and TNF-α), CXC
200 chemokines (CXCL-1, CXCL-2, IP-10, CXCL-11), and CC chemokines (CCL-2, CCL-4, CCL-
201 7, CCL-9, CCL-12, and CCL-22) in comparison to PMN incubated in mock-AT1 medium. These
202 findings demonstrated that PMN express proinflammatory cytokines and chemokines when
203 exposed to RCoV-infected epithelial cells. This is in agreement with the reduced concentrations
204 of chemokines in the BALF and cellular infiltration in the lungs of rats treated with αPMN
205 antibody compared to NRS-treated rats, during RCoV infection.

206

207 **The presence of PMN in the lungs is associated with tissue damage.**

208 Hemorrhagic lesions are observed on the surface of the lungs following the same kinetics
209 as PMN recruitment during RCoV infection (Funk *et al.*, 2009). Therefore, we determined
210 whether the presence of PMN correlated with visible lesions on the surface of rat lungs. RCoV
211 infection of NRS-treated rats resulted in gross pulmonary lesions in all animals that were
212 analyzed on day 4, and the majority of NRS-treated animals did not have lesions on day 8. The
213 presence of lesions on the lungs of NRS-treated animals corresponded to increased numbers of
214 PMN in the airways (Table 2). In contrast, none of the rats treated with αPMN throughout
215 infection had visible lesions, which corresponded to the absence of PMN in the BALF. Likewise,
216 in rats that received αPMN only early during infection (through day 2), no lesions were visible
217 on the lungs on day 4, when PMN were also not detected in the BALF. Late influx of PMN to

the respiratory tracts of transiently depleted rats by day 8 corresponded to the presence of pulmonary lesions in 5 of the 6 animals evaluated. In addition to surface lesions, we measured total protein in the BALF of rats as an indicator of damage to the epithelial barrier. When PMN were present in the BALF, there was a corresponding increase in protein concentration (Table 2). Furthermore, animals that had low numbers of PMN also had low total protein concentrations in the BALF. Collectively, these findings implicate PMN in causing tissue injury including gross hemorrhagic lesions and epithelial permeability.

Histological analysis was performed to compare lung pathology in PMN-depleted and NRS-treated rats during RCoV infection. Corresponding with focal areas of pneumonitis (Fig. 4a), NRS/RCoV rats had severe bronchiolar and peribronchiolar inflammation, necrosis, and epithelial sloughing (Fig. 6b), compared to mock-inoculated rats (Fig. 6a). Some alveoli of NRS/RCoV rats contained transudate fluid, dead cells, and inflammatory cells (Fig. 6e), compared to the clear alveoli of uninfected rats (Fig. 6d). Interestingly, most of this inflammation was resolved by day 8 (Fig. S2), with mainly foamy macrophages present in the alveoli. Although inflammatory cells were absent in αPMN-treated rats on day 4 post-infection, these animals had sloughing of dead epithelial cells in the bronchioles (Fig. 6c), and engorged alveolar capillaries (Fig. 6f). In summary, pulmonary RCoV infection resulted in strikingly different histopathology in NRS vs. αPMN treated rats. PMN-dependent responses were associated with focal pneumonitis, epithelial necrosis, edema, and vascular pathology, while the lack of PMN was associated with epithelial and vascular pathology.

Discussion

The activities of PMN during respiratory viral infections are complex and often dichotomous: contributing to both beneficial antiviral responses and detrimental pathology. We depleted PMN from rats during infection with a non-fatal respiratory coronavirus, RCoV, to determine their contributions to an effective antiviral response. In contrast to NRS-treated rats, rats that were treated with αPMN throughout or early during RCoV infection had increased mortality and morbidity and prolonged pulmonary viral replication. Further, PMN were required for the production of chemokines in the airways and infiltration of macrophages and lymphocytes into the lungs. These findings suggest that PMN are needed early during infection to elicit an effective cellular response to control viral replication and attenuate disease severity. Despite an effective response against RCoV, NRS-treated rats had pulmonary lesions, characterized by capillary congestion, hemorrhage, edema, and epithelial permeability. Taken together, these findings highlight the dichotomous roles of PMN by contributing to effective anti-viral responses, but also mediating tissue pathology.

A rabbit anti-rat PMN antibody was used to deplete PMN *in vivo* without significantly affecting circulating monocytes and lymphocytes. This antibody is widely used to deplete PMN in rats but most studies do not report the effects on other cell populations (Janardhan *et al.*, 2006; Li *et al.*, 2007; Ofulue & Ko, 1999; Sir *et al.*, 2000). Snipes *et al.* observed complete depletion of PMN and transiently reduced lymphocyte numbers in the blood of rats using this antibody (Snipes *et al.*, 1995). However, their study and others have demonstrated that αPMN does not reduce viability of other white blood cell types *in vitro* at the same concentration that inactivates PMN (Ofulue & Ko, 1999; Snipes *et al.*, 1995). We did not observe reduced lymphocyte numbers in αPMN-treated rats, but we used a lower dose of αPMN that was repeated every other day compared to a higher dose given once in the Snipes *et al*. study. In addition, differences in

the antibody lots and genetic lines and ages of the rats may be responsible for the differences in our studies. αPMN treatment alone resulted in early weight loss that was not statistically significant compared to NRS-treated rats. This was distinct from the prolonged, significant weight loss observed in the RCoV-infected αPMN treated rats. RCoV infection of PMN-depleted rats resulted in clinical signs consistent with infection by this viral strain, which corresponded with prolonged viral replication. However, we cannot exclude a role for potential secondary infections in exacerbating these findings.

Our study indicates that PMN are needed for effective clearance of pulmonary RCoV infection. PMN may have direct antiviral functions, including phagocytosis of viruses and virus-infected cells (Fujisawa, 2008; Hartshorn *et al.*, 1994; Hashimoto *et al.*, 2007; Tecle *et al.*, 2007; West *et al.*, 1987). PMN may also contribute to protection by recruitment and activation of other immune cell types (Beauvillain *et al.*, 2007; Radsak *et al.*, 2000; Scapini *et al.*, 2000). In previous studies, we showed that RCoV infects AT1 cells in the lungs and induces expression of chemokines that activate functional responses of PMN (Funk *et al.*, 2009; Miura *et al.*, 2007; Rzepka *et al.*, 2012). Here, we show that PMN responded to medium from RCoV-infected AT1-like cells *in vitro* by increasing mRNA levels of proinflammatory cytokines and chemokines. Further, depletion of PMN *in vivo* resulted in reduced concentrations of chemokines in the airways of RCoV-infected rats. Our *in vivo* findings suggest that PMN are a source of chemokines, including IP-10, CCL-2, CXCL-1, and CXCL-3, in the airways during RCoV infection. It is also possible that PMN induce other cell types to produce these chemokines. CXCL-1 and CXCL-3 recruit and activate PMN (Rzepka *et al.*, 2012; Shibata *et al.*, 1995). The decrease in these chemokines may explain the lack of PMN recruitment to the lungs after their numbers have returned to normal in the blood. CCL-2 mediates chemotaxis and activation of

macrophages. IP-10 recruits monocytes and lymphocytes and is critical for the recruitment of both $CD4^+$ and $CD8^+$ T cells in response to neurotropic murine coronavirus infection (Liu *et al.*, 2000). Histopathological and BALF analyses demonstrated robust cellular inflammation in the lungs and airways of RCoV-infected rats, which was dramatically absent in PMN-depleted rats. We specifically found reduced numbers of CD4+ and CD8+ cells in BALF from PMN-depleted animals. The numbers of circulating lymphocytes were not altered directly by αPMN treatment. Therefore, we hypothesize that the reduced numbers of lymphocytes in the respiratory tract of αPMN-treated rats was due to the absence of PMN. Others have shown that T cells are essential for effective clearance of RCoV (Weir *et al.*, 1990). Our data support a role for PMN in recruitment of T cells to the respiratory tract, which may be responsible for viral clearance.

In addition to providing protection from RCoV-mediated disease, we found that the presence of PMN in the lungs was associated with histopathology, hemorrhagic lesions, and increased epithelial permeability. While it seems contradictory that the animals with overt histopathology and lesions did not have severe clinical signs or mortality, this has been observed by other studies (Funk *et al.*, 2009; Wojcinski & Percy, 1986). A comprehensive study using the same RCoV strain (sialodacryoadentitis virus) found significant lesions in the lower respiratory tract, including gross lesions on the lungs and interstitial pneumonitis with PMN, epithelial necrosis, occluded alveoli, and edema (Wojcinski & Percy, 1986). Despite the dramatic macroscopic and microscopic pulmonary lesions, they only observed mild clinical signs. Like our findings, the lesions observed were focal in nature and were completely resolved by day 12 post-infection. Thus, healthy rats mount an inflammatory response to RCoV infection, associated with focal, transient lesions in the lung, which effectively limits disease severity. PMN,

macrophages, and lymphocytes are all present in these lesions and their individual roles have not been deciphered.

Experimental depletion of PMN in other coronavirus infection models has resulted in a range of outcomes, which may reflect their complex roles in both viral clearance and immunopathology. Infection of PMN-depleted mice with a neurotropic murine coronavirus, JHMV, causes increased viral titers in the brain and a more rapid decline to death compared to mice with PMN (Zhou *et al.*, 2003). Furthermore, when a CXCR2-specific antibody is used to prevent PMN recruitment to the brain during JHMV infection, mortality is increased with corresponding increases in viral titers in the brain (Hosking *et al.*, 2009). These studies suggest that PMN contribute to protection against JHMV replication and disease. In contrast, PMN depletion during infection with a recombinant JHM virus (RJHM) that induces robust recruitment of PMN to the brain, results in a slightly delayed time to death and reduced apoptosis in the brains of infected mice (Iacono *et al.*, 2006), suggesting that PMN contribute to pathology during RJHM. Finally, depletion of PMN in interferon alpha receptor knock-out (IFNAR-/-) mice, which are highly susceptible to infection by an attenuated strain of JHMV, does not affect viral replication or disease severity (Ireland *et al.*, 2008). Likewise, PMN depletion in mice infected with a hepatotropic murine coronavirus, MHV-A59, does not alter disease pathology (Cervantes-Barragan *et al.*, 2009). The contrasting roles of PMN during murine coronavirus infections are likely dependent upon the age and strain of mice and the relative virulence of the particular virus strains being studied. These parameters, which vary amongst the studies, may alter the balance between the protective and pathogenic functions of PMN.

Studies to determine the role of PMN in the pathogenesis of influenza virus infections have also generated disparate conclusions depending upon the dose and strain of virus, genetic

line of mice, and specificity of the depletion antibody for PMN. PMN depletion in mouse models of highly virulent influenza infections results in decreased disease severity, suggesting a role for PMN in pathogenesis (Bradley *et al.*, 2012; Crowe *et al.*, 2009; Sakai *et al.*, 2000). In contrast, other studies have found that depletion of PMN results in increased disease severity during influenza infection in mice, suggesting a protective role for PMN (Dienz *et al.*, 2012; Fujisawa, 2008; Tate *et al.*, 2008; Tate *et al.*, 2012; Tate *et al.*, 2009; Tate *et al.*, 2011; Tumpey *et al.*, 2005). These studies further reflect the complex, dichotomous functions of PMN during respiratory viral infections.

Many respiratory viruses cause significant morbidity without mortality in immunocompetent adults. Animal models that emulate non-fatal viral replication and pathology in the respiratory tract are critical to determine the components of immunity that protect against severe disease. RCoV infection of adult rats provides a valuable model for elucidating the mechanisms of effective immune responses to a pulmonary coronavirus infection in the natural host of the virus. Our findings demonstrate that although PMN are needed for effective resolution of RCoV infection, they contribute to lung pathology. A clear understanding of the interplay between beneficial and detrimental functions of PMN will lead to novel therapeutic strategies to reduce morbidity during respiratory viral infections.

Methods

Viruses and cell lines

RCoV strain sialodacryoadenitis virus was propagated and titrated by plaque assay in L2P41.a cells (Gagneten *et al.*, 1996) as described previously (Miura *et al.*, 2007). Virus and cell stocks were obtained from Dr. Kathryn Holmes (University of Colorado Denver, Aurora, CO).

PMN depletion and RCoV infection

Experiments were performed according to protocols approved by the University of Idaho Institutional Animal Care and Use Committee, following the Guide for the Care and Use of Laboratory Animals. Eight-week old male Fisher 344 rats (Harlan Laboratories Inc.) were used for infections. A pilot study was performed to determine the volume of rabbit anti-rat PMN serum (αPMN; Cedarlane) that effectively depleted circulating PMN without affecting monocyte and lymphocyte numbers. To deplete PMN through-out RCoV infection, rats were injected intraperitoneally with 300 µl of αPMN or normal rabbit serum (NRS) 1 day prior to infection and every 48 h thereafter (Fig. 1a). Six animals for each of the mock groups (NRS/mock and αPMN/mock), 10 NRS/RCoV, and 18 αPMN/RCoV treated rats were monitored for morbidity and mortality and surviving animals were euthanized on day 8 or 12 for tissue analyses. An additional 6 rats were included in the RCoV-infected groups (NRS/RCoV and αPMN/RCoV) and harvested on day 4. To obtain transient PMN depletion, rats were injected with serum on days -1 and +2 with respect to the infection (Fig. 3a). For transient depletion, 10 NRS/RCoV and 12 αPMN/RCoV rats were monitored for morbidity and mortality and the survivors were used for assays on day 8. An additional 5 rats per group were harvested on day 4. On day 0, rats were anesthetized with 80 mg ketamine ml^{-1} and 12 mg xylazine ml^{-1} and inoculated intranasally with

200 µl of RCoV (4-5 x 10^5 p.f.u.) or supernatant medium from mock-inoculated L2P-41a cells. Animals were weighed daily and those that lost more than 20% of their initial body were euthanized by an overdose of sodium pentobarbital, followed by exsanguination. Rats were monitored daily for clinical signs, including: 1) eye and nasal discharge, 2) lethargy, 3) sneezing or coughing, 4) ruffled fur, 5) hunched posture, 6) labored breathing, 7) visible swelling around the face and neck, 8) porphyrin stained eye secretions, 9) shaking, and 10) death. Based on the severity of these clinical signs, rats were scored on a scale of 0-8: healthy rats with no clinical signs received 0 points, rats with a combination of minor clinical signs received 1-3 points, more severe clinical signs 4-7 points, and dead animals received a clinical score of 8.

Blood and BALF analyses

BALF was collected from euthanized rats by flushing the lungs with 10 ml of saline 2-3 times. Cytospin preparations of BALF cells and blood smears were differentially stained with HEMA3 staining kit (Fisher Diagnostics). Cell-free BALF was used for quantification of protein by Bradford assay (Bio-Rad Laboratories) and chemokines by ELISAs (R&D Systems, Inc.; Thermo Scientific; Lifespan Biosciences Inc.).

Analysis of cytokine gene expression by PMN *in vitro*

Bone marrow PMN were isolated from uninfected rats as previously described (Rzepka *et al.*, 2012). Type 2 alveolar epithelial cells were isolated and trans-differentiated *in vitro* to AT1-like cells (Miura *et al.*, 2007; Rzepka *et al.*, 2012). AT1-like cells were infected with RCoV for

24 h and supernatant medium was collected (RCoV-AT1) and co-cultured with freshly purified PMN for 4 h. RNA was isolated from PMN and mRNA levels were quantified using Rat Inflammatory Cytokines and Receptors RT^{2}Profiler Arrays (SABiosciences/QIAGEN).

Lung virus titration

Lung tissues were weighed and homogenized in Dulbecco's Modified Eagle Medium with 50% FBS. Plaque assay in L2P41.a cells was performed to quantify the p.f.u. gram^{-1} of lung tissue (Miura *et al.*, 2007).

Histopathology

Lungs were fixed in 4% formaldehyde, dehydrated, embedded in paraffin, and sectioned. Embedding and sectioning were performed by Washington Animal Disease Diagnostic Laboratory at Washington State University (Pullman, WA). Tissue sections were de-paraffinized, stained with hematoxylin and eosin (Sigma Aldrich), and pathology was analyzed by a blinded pathologist (O.B.B.). Tissue sections were imaged using a Leica microscope equipped with a Nikon DS2 digital camera. Systematic uniform random sampling was performed on representative lung sections from three animals per group to photograph (at 20X magnification; 30-80 images per section) and count inflammatory cells per tissue area. Image J software(NIH) was used for cell quantification and measurement of numerical density (cells per unit area).

Flow cytometry

Cells from BALF were incubated with FITC-conjugated CD4, CD8, or isotype control antibodies (Biolegend, San Diego, CA). Ten thousand events per sample were collected using FACS-Aria (Becton Dickinson, Franklin Lakes, NJ) and data were analyzed using FlowJo version 7.6.5. (Tree Star, Inc., Ashland, OR). $CD4^+$ and $CD8^+$ T cells were gated from macrophages by side scatter profiles.

Statistical analysis

Statistical analyses were performed using GraphPad Prism, version 5.00 (GraphPad Software).

Acknowledgements

This work was supported by a Career Development Award from the Pacific Northwest Regional Center of Excellence (NIH/NIAID: U54 AI081680), by grant P20 RR015587 from the National Center for Research Resources (NCRR), a component of the NIH, and by grant P20 RR0116454 from the INBRE Program of the NCRR. The authors would like to thank Dr. Kathryn Holmes, University of Colorado Denver, for cell lines and virus stocks, Ms. Ann Norton for assistance with microscopy and Dr. Craig Miller for assistance with analysis.

References

Assiri, A., Al-Tawfiq, J. A., Al-Rabeeah, A. A., Al-Rabiah, F. A., Al-Hajjar, S., Al-Barrak, A., Flemban, H., Al-Nassir, W. N., Balkhy, H. H., Al-Hakeem, R. F., Makhdoom, H. Q., Zumla, A. I. & Memish, Z. A. (2013). Epidemiological, demographic, and clinical characteristics of 47 cases of Middle East respiratory syndrome coronavirus disease from Saudi Arabia: a descriptive study. *The Lancet infectious diseases* 13, 752-761.

Beauvillain, C., Delneste, Y., Scotet, M., Peres, A., Gascan, H., Guermonprez, P., Barnaba, V. & Jeannin, P. (2007). Neutrophils efficiently cross-prime naive T cells in vivo. *Blood* 110, 2965-2973.

Bradley, L. M., Douglass, M. F., Chatterjee, D., Akira, S. & Baaten, B. J. (2012). Matrix metalloprotease 9 mediates neutrophil migration into the airways in response to influenza virus-induced toll-like receptor signaling. *PLoS Pathog* 8, e1002641.

Cervantes-Barragan, L., Kalinke, U., Zust, R., Konig, M., Reizis, B., Lopez-Macias, C., Thiel, V. & Ludewig, B. (2009). Type I IFN-mediated protection of macrophages and dendritic cells secures control of murine coronavirus infection. *J Immunol* 182, 1099-1106.

Crowe, C. R., Chen, K., Pociask, D. A., Alcorn, J. F., Krivich, C., Enelow, R. I., Ross, T. M., Witztum, J. L. & Kolls, J. K. (2009). Critical Role of IL-17RA in Immunopathology of Influenza Infection. *The Journal of Immunology* 183, 5301-5310.

Denlinger, L. C., Sorkness, R. L., Lee, W. M., Evans, M. D., Wolff, M. J., Mathur, S. K., Crisafi, G. M., Gaworski, K. L., Pappas, T. E., Vrtis, R. F., Kelly, E. A., Gern, J. E. & Jarjour, N. N. (2011). Lower airway rhinovirus burden and the seasonal risk of asthma exacerbation. *Am J Respir Crit Care Med* 184, 1007-1014.

Dienz, O., Rud, J. G., Eaton, S. M., Lanthier, P. A., Burg, E., Drew, A., Bunn, J., Suratt, B. T., Haynes, L. & Rincon, M. (2012). Essential role of IL-6 in protection against H1N1 influenza virus by promoting neutrophil survival in the lung. *Mucosal immunology* 5, 258-266.

Fujisawa, H. (2008). Neutrophils play an essential role in cooperation with antibody in both protection against and recovery from pulmonary infection with influenza virus in mice. *J Virol* 82, 2772-2783.

Funk, C. J., Manzer, R., Miura, T. A., Groshong, S. D., Ito, Y., Travanty, E. A., Leete, J., Holmes, K. V. & Mason, R. J. (2009). Rat respiratory coronavirus infection: replication in airway and alveolar epithelial cells and the innate immune response. *J Gen Virol* 90, 2956-2964.

Gagneten, S., Scanga, C. A., Dveksler, G. S., Beauchemin, N., Percy, D. & Holmes, K. V. (1996). Attachment glycoproteins and receptor specificity of rat coronaviruses. *Lab Anim Sci* 46, 159-166.

Gaunt, E. R., Hardie, A., Claas, E. C., Simmonds, P. & Templeton, K. E. (2010). Epidemiology and clinical presentations of the four human coronaviruses 229E, HKU1, NL63, and OC43 detected over 3 years using a novel multiplex real-time PCR method. *Journal of clinical microbiology* 48, 2940-2947.

Grommes, J. & Soehnlein, O. (2011). Contribution of neutrophils to acute lung injury. *Mol Med* 17, 293-307.

Hartshorn, K. L., Crouch, E. C., White, M. R., Eggleton, P., Tauber, A. I., Chang, D. & Sastry, K. (1994). Evidence for a protective role of pulmonary surfactant protein D (SP-D) against influenza A viruses. *J Clin Invest* 94, 311-319.

Hashimoto, Y., Moki, T., Takizawa, T., Shiratsuchi, A. & Nakanishi, Y. (2007). Evidence for phagocytosis of influenza virus-infected, apoptotic cells by neutrophils and macrophages in mice. *J Immunol* 178, 2448-2457.

Hosking, M. P., Liu, L., Ransohoff, R. M. & Lane, T. E. (2009). A protective role for ELR+ chemokines during acute viral encephalomyelitis. *PLoS Pathog* 5, e1000648.

Iacono, K. T., Kazi, L. & Weiss, S. R. (2006). Both spike and background genes contribute to murine coronavirus neurovirulence. *J Virol* 80, 6834-6843.

Ireland, D. D., Stohlman, S. A., Hinton, D. R., Atkinson, R. & Bergmann, C. C. (2008). Type I interferons are essential in controlling neurotropic coronavirus infection irrespective of functional CD8 T cells. *J Virol* 82, 300-310.

Janardhan, K. S., Sandhu, S. K. & Singh, B. (2006). Neutrophil depletion inhibits early and late monocyte/macrophage increase in lung inflammation. *Frontiers in bioscience : a journal and virtual library* 11, 1569-1576.

Khanolkar, A., Hartwig, S. M., Haag, B. A., Meyerholz, D. K., Harty, J. T. & Varga, S. M. (2009). Toll-like receptor 4 deficiency increases disease and mortality after mouse hepatitis virus type 1 infection of susceptible C3H mice. *J Virol* 83, 8946-8956.

Lee, N., Hui, D., Wu, A., Chan, P., Cameron, P., Joynt, G. M., Ahuja, A., Yung, M. Y., Leung, C. B., To, K. F., Lui, S. F., Szeto, C. C., Chung, S. & Sung, J. J. (2003). A major outbreak of severe acute respiratory syndrome in Hong Kong. *The New England journal of medicine* 348, 1986-1994.

Leong, H. N., Earnest, A., Lim, H. H., Chin, C. F., Tan, C. S., Puhaindran, M. E., Tan, A. C., Chen, M. I. & Leo, Y. S. (2006). SARS in Singapore--predictors of disease severity. *Annals of the Academy of Medicine, Singapore* 35, 326-331.

Li, X., Kovacs, E. J., Schwacha, M. G., Chaudry, I. H. & Choudhry, M. A. (2007). Acute alcohol intoxication increases interleukin-18-mediated neutrophil infiltration and lung inflammation following burn injury in rats. *American journal of physiology Lung cellular and molecular physiology* 292, L1193-1201.

Liu, M. T., Chen, B. P., Oertel, P., Buchmeier, M. J., Armstrong, D., Hamilton, T. A. & Lane, T. E. (2000). The T cell chemoattractant IFN-inducible protein 10 is essential in host defense against viral-induced neurologic disease. *J Immunol* 165, 2327-2330.

Mantovani, A., Cassatella, M. A., Costantini, C. & Jaillon, S. (2011). Neutrophils in the activation and regulation of innate and adaptive immunity. *Nature reviews Immunology* 11, 519-531.

McKean, M. C., Hewitt, C., Lambert, P. C., Myint, S. & Silverman, M. (2003). An adult model of exclusive viral wheeze: inflammation in the upper and lower respiratory tracts. *Clin Exp Allergy* 33, 912-920.

Miura, T. A., Wang, J., Holmes, K. V. & Mason, R. J. (2007). Rat coronaviruses infect rat alveolar type I epithelial cells and induce expression of CXC chemokines. *Virology* 369, 288-298.

Nagata, N., Iwata, N., Hasegawa, H., Fukushi, S., Harashima, A., Sato, Y., Saijo, M., Taguchi, F., Morikawa, S. & Sata, T. (2008). Mouse-passaged severe acute respiratory syndrome-associated coronavirus leads to lethal pulmonary edema and diffuse alveolar damage in adult but not young mice. *The American journal of pathology* 172, 1625-1637.

Ofulue, A. F. & Ko, M. (1999). Effects of depletion of neutrophils or macrophages on development of cigarette smoke-induced emphysema. *The American journal of physiology* 277, L97-105.

Radsak, M., Iking-Konert, C., Stegmaier, S., Andrassy, K. & Hansch, G. M. (2000). Polymorphonuclear neutrophils as accessory cells for T-cell activation: major histocompatibility complex class II restricted antigen-dependent induction of T-cell proliferation. *Immunology* 101, 521-530.

Rzepka, J. P., Haick, A. K. & Miura, T. A. (2012). Virus-infected alveolar epithelial cells direct neutrophil chemotaxis and inhibit their apoptosis. *Am J Respir Cell Mol Biol* 46, 833-841.

Sakai, S., Kawamata, H., Mantani, N., Kogure, T., Shimada, Y., Terasawa, K., Sakai, T., Imanishi, N. & Ochiai, H. (2000). Therapeutic Effect of Anti-Macrophage Inflammatory Protein 2 Antibody on Influenza Virus-Induced Pneumonia in Mice. *Journal of Virology* 74, 2472-2476.

Scapini, P., Lapinet-Vera, J. A., Gasperini, S., Calzetti, F., Bazzoni, F. & Cassatella, M. A. (2000). The neutrophil as a cellular source of chemokines. *Immunol Rev* 177, 195-203.

Shibata, F., Konishi, K., Kato, H., Komorita, N., al-Mokdad, M., Fujioka, M. & Nakagawa, H. (1995). Recombinant production and biological properties of rat cytokine-induced neutrophil chemoattractants, GRO/CINC-2 alpha, CINC-2 beta and CINC-3. *Eur J Biochem* 231, 306-311.

Siemsen, D. W., Schepetkin, I. A., Kirpotina, L. N., Lei, B. & Quinn, M. T. (2007). Neutrophil isolation from nonhuman species. *Methods Mol Biol* 412, 21-34.

Sir, O., Fazal, N., Choudhry, M. A., Gamelli, R. L. & Sayeed, M. M. (2000). Neutrophil depletion prevents intestinal mucosal permeability alterations in burn-injured rats. *Am J Physiol Regul Integr Comp Physiol* 278, R1224-1231.

Snipes, M. B., Barnett, A. L., Harkema, J. R., Hotchkiss, J. A., Rebar, A. H. & Reddick, L. J. (1995). Specific biological effects of an anti-rat PMN antiserum intraperitoneally infected into f344/n rats. *Veterinary clinical pathology / American Society for Veterinary Clinical Pathology* 24, 11-17.

Tate, M. D., Brooks, A. G. & Reading, P. C. (2008). The role of neutrophils in the upper and lower respiratory tract during influenza virus infection of mice. *Respir Res* 9, 57.

Tate, M. D., Brooks, A. G., Reading, P. C. & Mintern, J. D. (2012). Neutrophils sustain effective CD8(+) T-cell responses in the respiratory tract following influenza infection. *Immunology and cell biology* 90, 197-205.

Tate, M. D., Deng, Y. M., Jones, J. E., Anderson, G. P., Brooks, A. G. & Reading, P. C. (2009). Neutrophils ameliorate lung injury and the development of severe disease during influenza infection. *J Immunol* 183, 7441-7450.

Tate, M. D., Ioannidis, L. J., Croker, B., Brown, L. E., Brooks, A. G. & Reading, P. C. (2011). The role of neutrophils during mild and severe influenza virus infections of mice. *PLoS ONE* 6, e17618.

Tecle, T., White, M. R., Gantz, D., Crouch, E. C. & Hartshorn, K. L. (2007). Human neutrophil defensins increase neutrophil uptake of influenza A virus and bacteria and modify virus-induced respiratory burst responses. *J Immunol* 178, 8046-8052.

Tsui, P. T., Kwok, M. L., Yuen, H. & Lai, S. T. (2003). Severe acute respiratory syndrome: clinical outcome and prognostic correlates. *Emerging infectious diseases* 9, 1064-1069.

Tumpey, T. M., Garcia-Sastre, A., Taubenberger, J. K., Palese, P., Swayne, D. E., Pantin-Jackwood, M. J., Schultz-Cherry, S., Solorzano, A., Van Rooijen, N., Katz, J. M. & Basler, C. F. (2005). Pathogenicity of influenza viruses with genes from the 1918 pandemic virus: functional roles of alveolar macrophages and neutrophils in limiting virus replication and mortality in mice. *J Virol* 79, 14933-14944.

Weir, E. C., Jacoby, R. O., Paturzo, F. X., Johnson, E. A. & Ardito, R. B. (1990). Persistence of sialodacryoadenitis virus in athymic rats. *Lab Anim Sci* 40, 138-143.
West, B. C., Eschete, M. L., Cox, M. E. & King, J. W. (1987). Neutrophil uptake of vaccinia virus in vitro. *J Infect Dis* 156, 597-606.
Widegren, H., Andersson, M., Borgeat, P., Flamand, L., Johnston, S. & Greiff, L. (2011). LTB4 increases nasal neutrophil activity and conditions neutrophils to exert antiviral effects. *Respiratory medicine* 105, 997-1006.
Wojcinski, Z. W. & Percy, D. H. (1986). Sialodacryoadenitis virus-associated lesions in the lower respiratory tract of rats. *Vet Pathol* 23, 278-286.
Zhou, J., Stohlman, S. A., Hinton, D. R. & Marten, N. W. (2003). Neutrophils promote mononuclear cell infiltration during viral-induced encephalitis. *J Immunol* 170, 3331-3336.

Figure Legends

Fig. 1. αPMN treatment depletes circulating PMN and increases disease severity during RCoV infection of rats.

(a) Rats were injected with αPMN or normal rabbit serum (NRS) intraperitoneally 1 day prior to intranasal inoculation with RCoV or medium (mock), and every 48 h thereafter. (b) Blood was collected from 3-5 animals per group daily to monitor white blood cell populations. Rats were monitored for mortality (c), body weight (d), and clinical signs of disease (e). Data are the mean values ± standard error from 6-18 rats per treatment per day (See key). Statistically significant differences between αPMN- and NRS-treated rats were identified using one-way ANOVA followed by the Newman-Keuls post-test: ** $p<0.01$; *** $p<0.001$.

Fig. 2. αPMN treatment reduces PMN recruitment and prolongs viral replication in the lungs.

Rats were injected with αPMN or NRS intraperitoneally 1 day prior to intranasal inoculation with RCoV, and every 48 h thereafter (see Fig. 1a). (a) Cells from bronchoalveolar lavage fluid

(BALF) were Giemsa-Wright stained and PMN were quantified morphologically. (b) Lung tissues were homogenized and viral titers were determined by plaque assay. Data are the mean values ± standard errors from 3-5 rats per group. Statistically significant differences between αPMN- and NRS-treated rats were identified using an unpaired t-test: ** $p<0.01$, *** $p<0.001$.

Fig. 3. PMN are needed early during RCoV infection to be protective.

(a) Rats were injected with αPMN or NRS serum intraperitoneally 1 day prior to and 2 days after intranasal inoculation with RCoV and analyzed on days 4 and 8 (arrows). (b) Cells from BALF of 3-5 rats per group were Giemas-Wright stained and PMN were quantified morphologically. (c) Lungs from 3-6 rats per group were homogenized and viral titers were determined by plaque assay. The data are mean values ± standard errors. Rats (see key for numbers) were monitored for (d) survival (p=0.046) and (e) weight loss. Statistically significant differences between αPMN- and NRS-treated rats were identified using (e) two-way ANOVA followed by a Bonferroni post-test or (b and c)unpaired t-test: *** $p<0.001$.

Fig. 4. PMN promote cellular inflammation in the lungs upon RCoV infection.

Rats were injected with αPMN or NRS intraperitoneally 1 day prior to intranasal inoculation with RCoV, and every 48 h thereafter. On day 4 after RCoV infection, (a) lungs were formaldehyde-fixed and paraffin-embedded, and hematoxylin and eosin stained sections were analyzed for cellular inflammation. Representative tissues from 3 animals per group are shown at 2X (top panels), 20X (middle panels) and 40X (bottom panels) magnification. Examples of cell types at 40X: # neutrophil, * macrophage, and ^ lymphocyte are indicated. (b) Density indices of inflammatory cells were quantified in lung sections from three animals per group using Image

J software. (c) White blood cells in BALF were quantified by Wright-Giemsa staining, and (d) lymphocyte subtypes by flow cytometry, using 4-6 animals per group. Statistically significant differences compared to NRS/RCoV-treated rats were identified using one-way ANOVA followed by the Newman-Keuls post-test: * $p<0.05$; ** $p<0.01$; *** $p<0.001$.

Fig. 5. αPMN-treated rats have reduced concentrations of chemokines in the airways during RCoV infection.

ELISAs were used to quantify the concentrations of (a) PMN specific (CXCL-1 and CXCL-3) and (b) monocyte and lymphocyte specific (IP-10 and CCL2) chemokines in BALF from αPMN- and NRS-treated rats after infection with RCoV or mock-inoculation. The data are mean values ± standard error from 3-5 rats per treatment. Statistically significant differences between αPMN- and NRS-treated rats were identified using one-way ANOVA followed by the Newman-Keuls post-test: ** $p<0.01$; *** $p<0.001$.

Fig. 6. Differential pathology in PMN-depleted vs. NRS-treated rats during RCoV infection.

Images of representative lung sections from 3 animals per treatment: (a,d) αPMN-treated/mock-inoculated, (b,e) NRS-treated/RCoV-infected, and (c,f) αPMN-treated/RCoV-infected showing histopathology on day 4 post-infection. αPMN/mock rats had normal terminal (TBr) and respiratory (RBr) bronchioles and alveoli (A). Lungs of NRS/RCoV rats had peribronchiolar inflammation with sloughing off of bronchiolar epithelium (†) and alveoli (A) filled with inflammatory cells and necrotic cell debris. Transudate-filled alveoli indicating alveolar edema (E) were diffusely distributed in the lesions and congested capillaries (arrows) were found

throughout the sections. αPMN/RCoV rats had mild pathology with sloughing off of bronchiolar epithelium (†), and congested capillaries (arrows).

Tables

Table 1. Cytokine and chemokine mRNAs with increased abundance in PMN exposed to medium from RCoV-infected, compared to mock-infected AT1 cells *in vitro*.

PMN were isolated from rat bone marrow and incubated for 4 h in conditioned medium from RCoV-infected or mock-inoculated AT1-like cells. RNA was isolated from the PMN and analyzed using quantitative RT-PCR arrays (SABiosciences) specific for proinflammatory cytokines and chemokines.

	Fold Induction of mRNA†		
Cytokine/Chemokine*	**Experiment 1**	**Experiment 2**	**Experiment 3**
CCL-2	18.0	19.9	1.8
CCL-4	5.5	4.0	2.7
CCL-7	73.3	40.4	11.1
CCL-9	7.9	8.3	4.5
CCL-12	10.1	1.4	94.9
CCL-22	5.8	16.5	3.4
CXCL-1	39.9	19.6	10.3
IP-10	4.9	17.2	3.1
CXCL-11	35.1	159.3	17.4
CXCL-2	13.8	23.2	8.7
CX3CL-1	4.5	2.3	1.9
IL-18	1.8	2.3	2.6
IL-1α	345.0	190.5	10.3
IL-1β	5.0	13.1	3.5
TNF-α	13.5	9.8	7.8

*Cytokine and chemokine mRNAs that were differentially expressed in at least two of three independent experiments.

† Values are fold difference in PMN incubated in medium from RCoV-infected compared to mock-inoculated AT1-like cells.

Table 2. The presence of PMN in the lungs of RCoV-infected rats corresponds to tissue damage.

Rats were treated with αPMN or NRS throughout (See Fig. 1a) or early (See Fig. 3a) during infection with RCoV. Cells from BALF were Wright-Giemsa stained and quantified morphologically. The number of rats with gross lesions on the lungs was recorded. Total protein in BALF was quantified by Bradford assay.

Treatment	% PMN in BALF[†]	Rats with gross lung lesions positive/total[#]	BALF protein[†] [mg/ml]
NRS Mock	0.0 (0.0)	0/6	0.8 (0.1)
NRS RCoV day 4	22.1 (1.3)***	5/5 (p=0.0011)	16.1 (3.3)**
NRS RCoV day 8	1.3 (0.7)	1/5	1.8 (1.3)
αPMN Mock	2.3 (2.0)	0/6	0.9 (0.3)
αPMN RCoV day 4	0.6 (0.6)	0/5	0.5 (0.2)
αPMN RCoV day 8	3.5 (1.1)	0/5	2.3 (0.9)
Early NRS Mock	6.8 (5.8)	0/6	0.3 (0.2)
Early NRS RCoV day 4	24.9 (3.2)**	4/5 (p=0.0094)	4.7 (0.7)***
Early NRS RCoV day 8	5.6 (1.2)	1/6	1.1 (0.2)
Early αPMN Mock	2.3 (0.6)	0/4	2.8 (1.0)
Early αPMN RCoV day 4	0.0 (0.0)	0/5	1.3 (0.3)
Early αPMN RCoV day 8	28.2 (1.9)***	5/6 (p=0.0126)	8.3 (1.6)**

[†]Values are the means of 4-6 rats per group with standard error in parentheses. Asterisks indicate statistically significant differences compared to mock for each group as determined by one-way ANOVA with Newman-Keuls post-test: **p<0.005, ***p<0.0001.

[#](p values) are given for groups that differ significantly from the mock for each group as determined by a likelihood ratio test.

Fig. 1

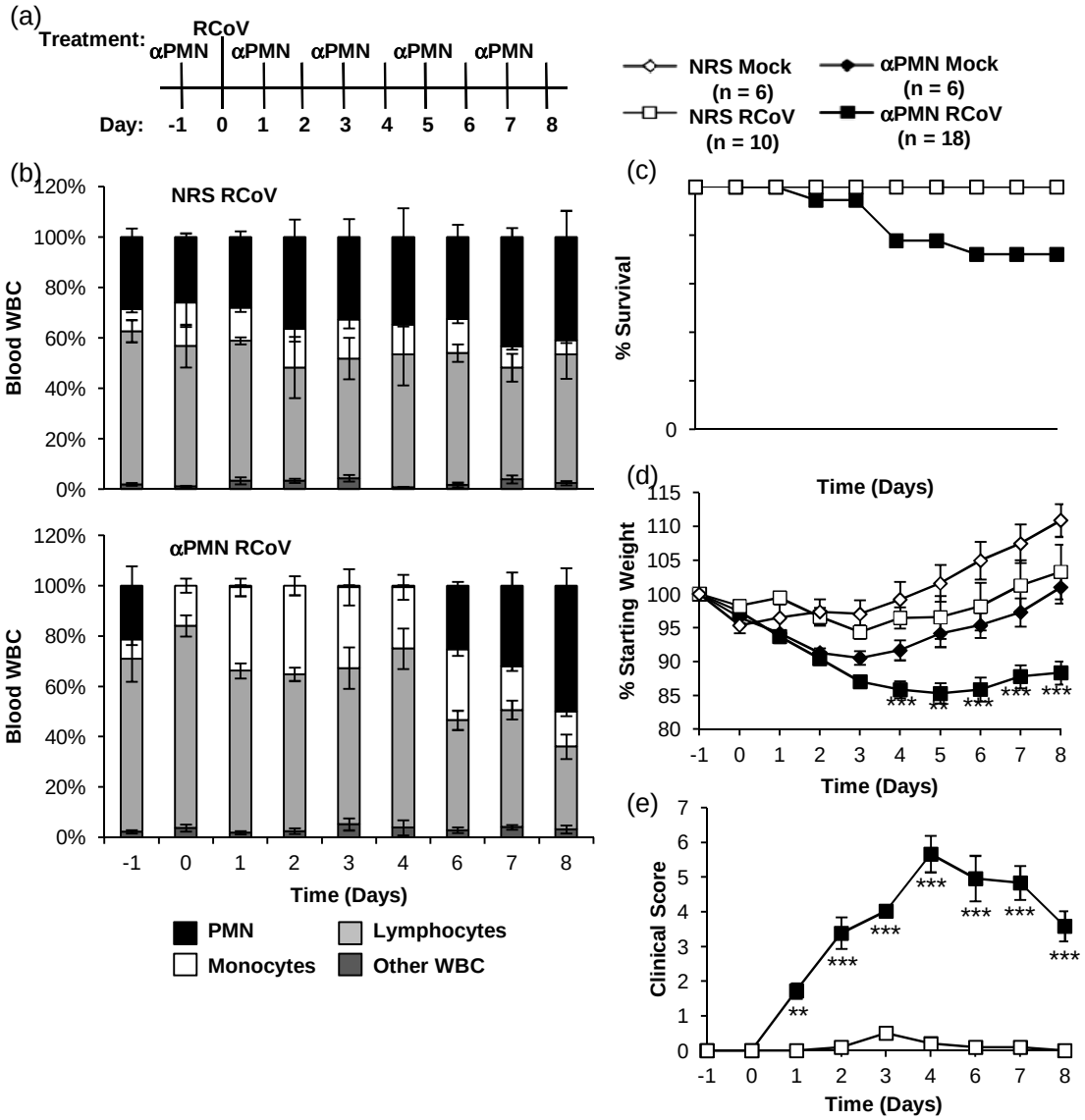
(a)
Treatment:
RCoV
αPMN
αPMN
αPMN
αPMN
αPMN
Day: -1 0 1 2 3 4 5 6 7 8
(b)
NRS RCoV
αPMN RCoV
Blood WBC
120%
100%
80%
60%
40%
20%
0%
-1 0 1 2 3 4 6 7 8
Time (Days)
PMN
Lymphocytes
Monocytes
Other WBC
NRS Mock (n = 6)
αPMN Mock (n = 6)
NRS RCoV (n = 10)
αPMN RCoV (n = 18)
(c)
% Survival
0
(d)
Time (Days)
% Starting Weight
115
110
105
100
95
90
85
80
-1 0 1 2 3 4 5 6 7 8
Time (Days)
(e)
Clinical Score
7
6
5
4
3
2
1
0
-1 0 1 2 3 4 6 7 8
Time (Days)

Fig. 2

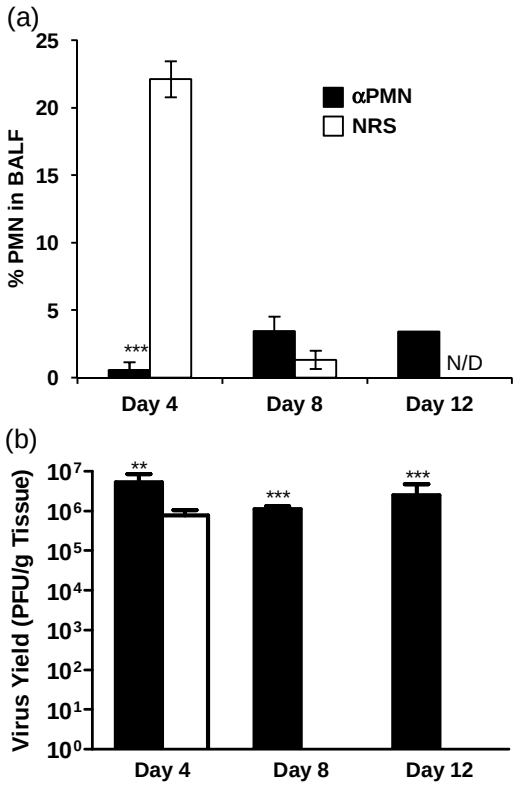
(a)
% PMN in BALF
25
20
15
10
5
0
αPMN
NRS
***
N/D
Day 4
Day 8
Day 12
(b)
Virus Yield (PFU/g Tissue)
10^7
10^6
10^5
10^4
10^3
10^2
10^1
10^0
**
***
***
Day 4
Day 8
Day 12

Fig. 3

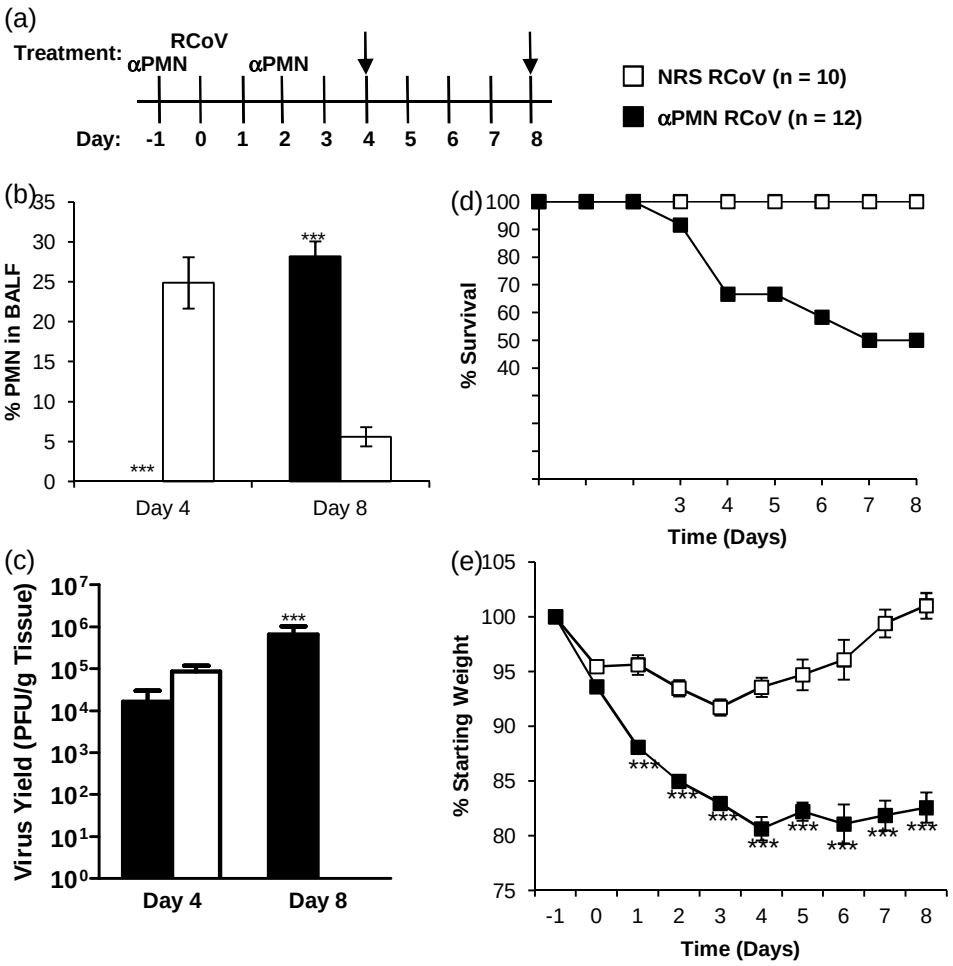
(a)
Treatment:
RCoV
αPMN
αPMN
Day: -1 0 1 2 3 4 5 6 7 8
NRS RCoV (n = 10)
αPMN RCoV (n = 12)
(b)
% PMN in BALF
Day 4
Day 8
(d)
% Survival
Time (Days)
(c)
Virus Yield (PFU/g Tissue)
Day 4
Day 8
(e)
% Starting Weight
Time (Days)

Fig. 4

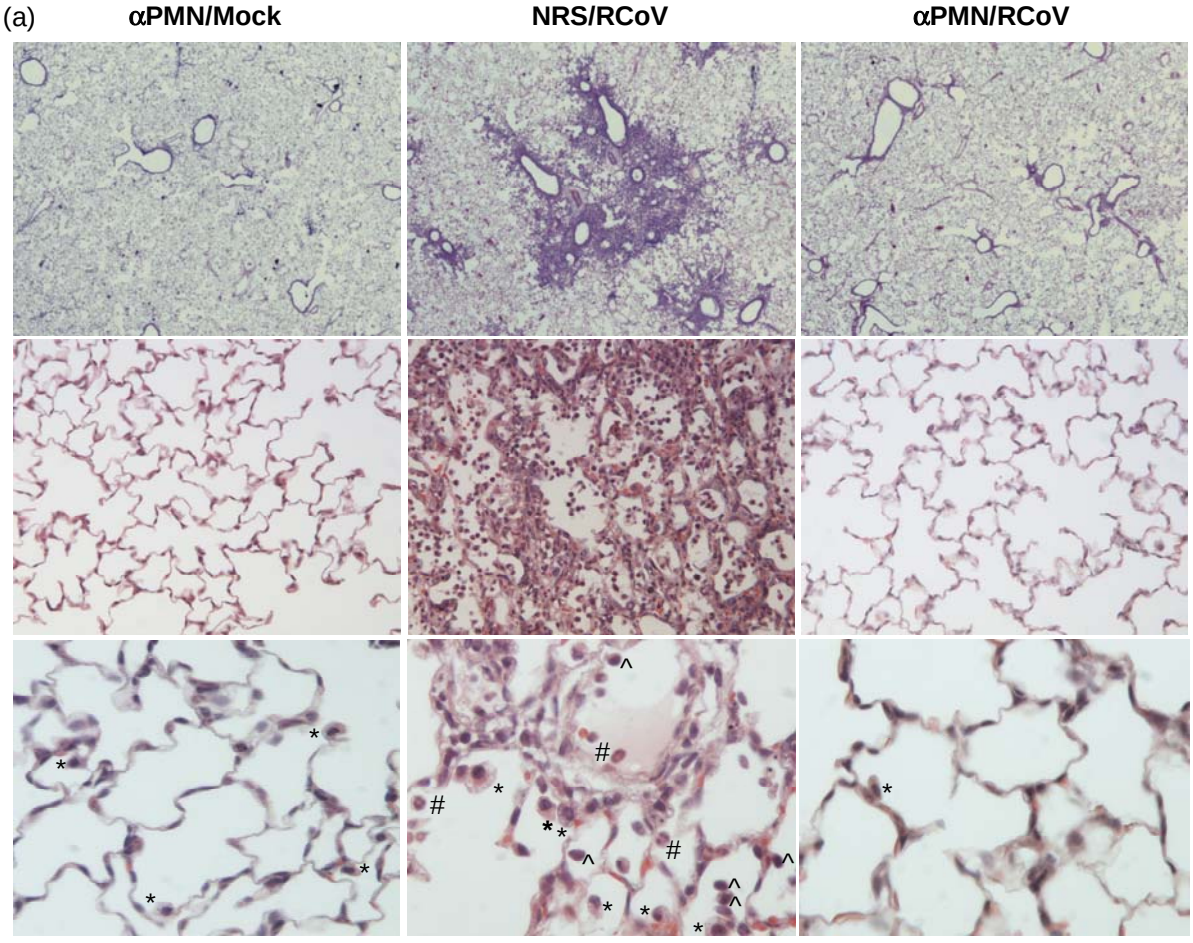
(a)
αPMN/Mock
NRS/RCoV
αPMN/RCoV

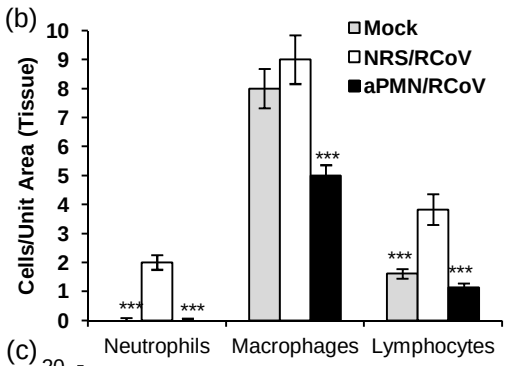
(b)
Mock
NRS/RCoV
aPMN/RCoV
Cells/Unit Area (Tissue)
Neutrophils
Macrophages
Lymphocytes

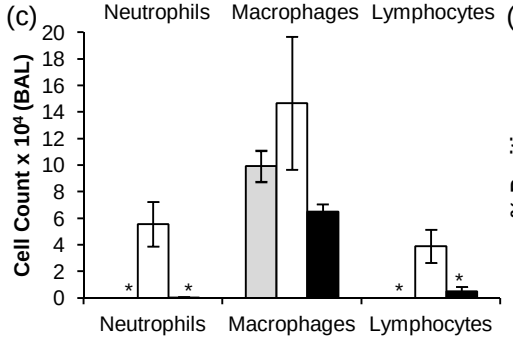
(c)
Cell Count x 10⁴ (BAL)
Neutrophils
Macrophages
Lymphocytes

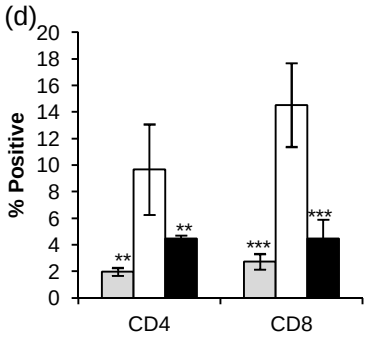
(d)
% Positive
CD4
CD8

Fig. 5

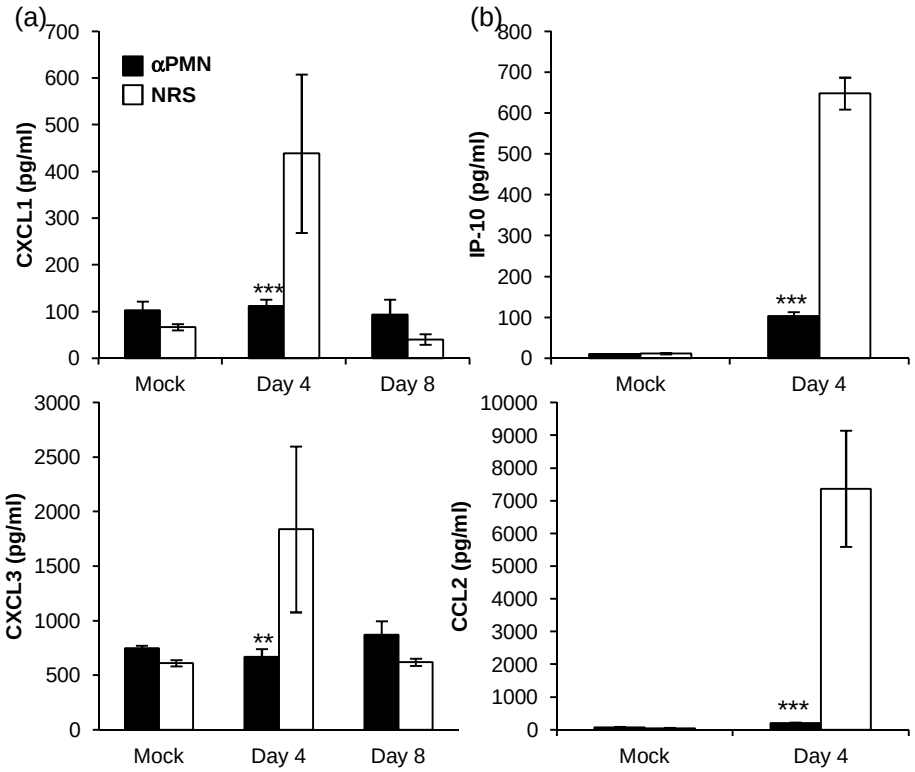
(a)
αPMN
NRS
CXCL1 (pg/ml)
0
100
200
300
400
500
600
700
***
Mock
Day 4
Day 8
CXCL3 (pg/ml)
0
500
1000
1500
2000
2500
3000
**
Mock
Day 4
Day 8
(b)
IP-10 (pg/ml)
0
100
200
300
400
500
600
700
800
***
Mock
Day 4
CCL2 (pg/ml)
0
1000
2000
3000
4000
5000
6000
7000
8000
9000
10000
***
Mock
Day 4

Fig. 6

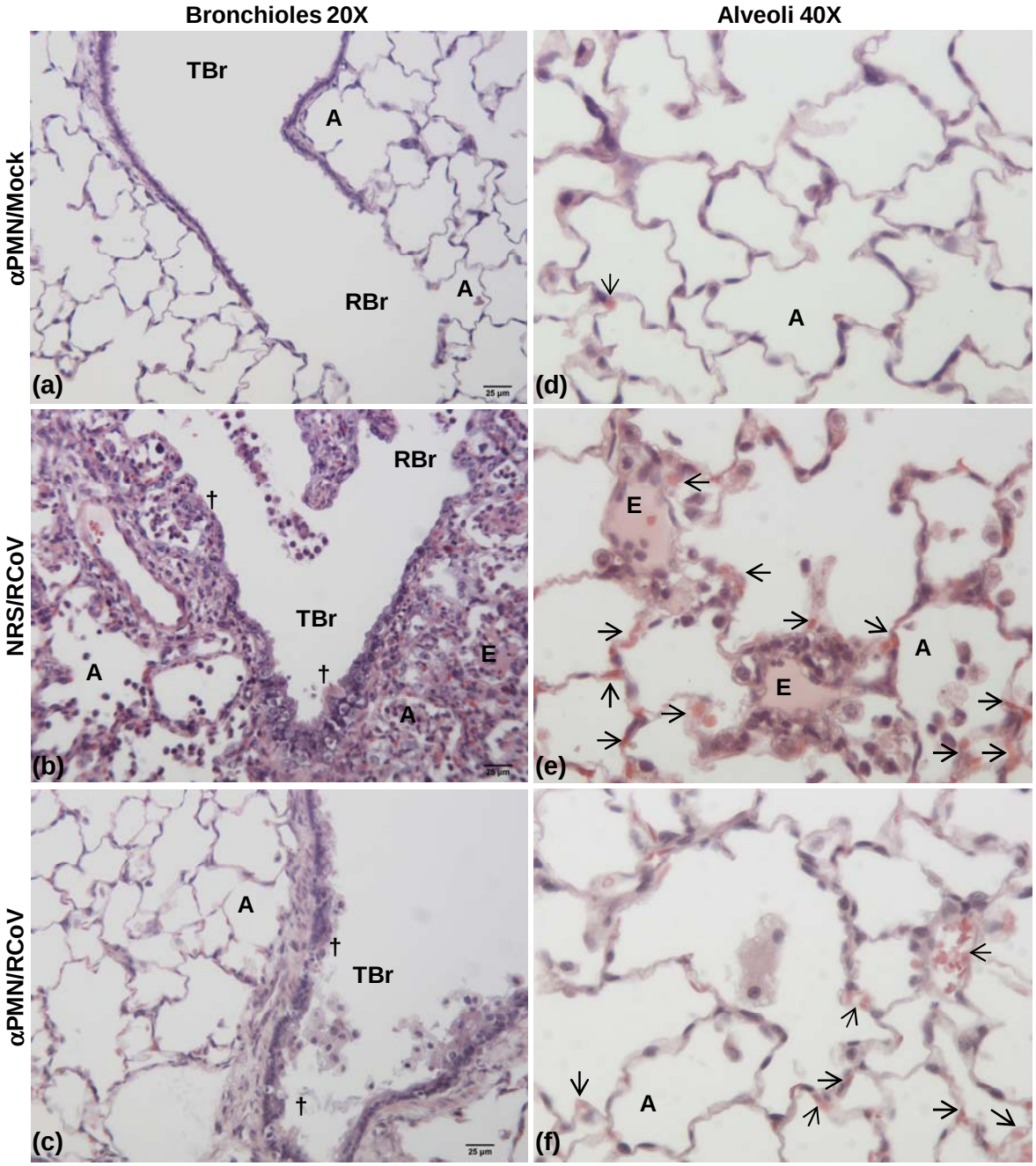
Bronchioles 20X
Alveoli 40X
αPMN/Mock
NRS/RCoV
αPMN/RCoV
TBr
A
RBr
E
†
(a)
(b)
(c)
(d)
(e)
(f)
25 µm